



Contents lists available at ScienceDirect

Spectrochimica Acta Part A: Molecular and Biomolecular Spectroscopy

journal homepage: www.elsevier.com/locate/saa

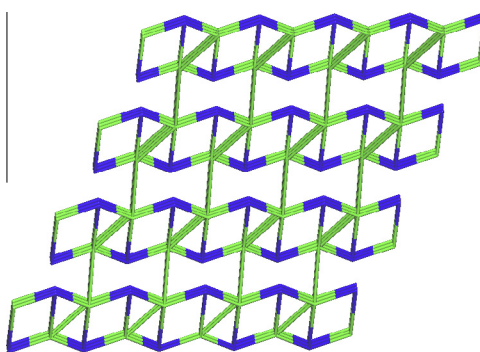
Synthesis, crystal structures, luminescence properties of two metal coordination polymers derived from 5-substituted isophthalate and flexible bis (triazole) ligands

Chun-lun Ming^a, Li-na Wang^a, Kristof Van Hecke^b, Guang-hua Cui^{a,*}^a College of Chemical Engineering, Hebei United University, 46 West Xinhua Road, Tangshan 063009, Hebei, PR China^b Department of Inorganic and Physical Chemistry, Ghent University, Krijgslaan 281 S3, B-9000 Ghent, Belgium

HIGHLIGHTS

- Two new metal coordination polymers have been synthesized.
- IR, PXRD, TG technique for the polymers.
- X-ray single-crystal structure analyses and discussion for two polymers.
- Luminescence properties of two complexes have been investigated.

GRAPHICAL ABSTRACT



ARTICLE INFO

Article history:

Received 17 December 2013
 Received in revised form 4 March 2014
 Accepted 18 March 2014
 Available online 27 March 2014

Keywords:

Crystal structure
 Bis (triazole) ligand
 Metal–organic framework
 Luminescence

ABSTRACT

Two new metal complexes, $[\text{Ni}(\text{btx})(\text{nip})(\text{H}_2\text{O})]_n$ (**1**), $\{[\text{Cd}(\text{btx})(\text{mip})(\text{H}_2\text{O})] \cdot \text{H}_2\text{O}\}_n$ (**2**) (btx = 1,4-bis(1,2,4-triazol-1-ylmethyl)benzene, H_2nip = 5-nitroisophthalic acid, H_2mip = 5-methyisophthalic acid) were synthesized under hydrothermal conditions and characterized by single-crystal X-ray diffraction methods, IR spectroscopy, TGA and elemental analysis. Complex **1** features a 3D metal-organic framework with three-fold interpenetrating CdSO_4 -type topology. Complex **2** exhibits a 2D network with square grid units, which is further extended into a rare **3,5T1** three-dimensional supramolecular network via three modes of classical $\text{O} \cdots \text{H} \cdots \text{O}$ hydrogen bonds. In addition, luminescence properties of **1** and **2** have also been investigated in the solid state.

© 2014 Elsevier B.V. All rights reserved.

Introduction

Metal organic coordination polymers (MOCPs) assembled from the linkage of metal center atoms through organic ligands have vital applications in luminescent devices, gas storage, ion exchange, separations, biomedicine, catalysis and so on [1–6]. In order to get

such intriguing topologies and functional materials, the crucial step is to employ appropriate organic building blocks as well as metal ions. However, construction of MOCPs with expected structures and properties in hydrothermal reactions is still a challenge, owing to the fact that the assembly of such complexes can be easily influenced by the geometrical and electronic properties of metal ions and ligands, temperature, pH value of the solution, etc. In recent years, 1,2,4-triazole and its derivatives have often been chosen as ligands for the construction of interesting and

* Corresponding author. Tel.: +86 0315 2592169; fax: +86 0315 2592170.

E-mail address: tscghua@126.com (G.-h. Cui).

fascinating structures [7–11]. Especially, the flexible 1,4-bis(1,2,4-triazol-1-ylmethyl)-benzene (btx) not only possesses the merits of triazole, but can also freely bend and rotate to interact with metal ions. [12–14]. A series of Cd–btx complexes with the third-order NLO (nonlinear optics) properties and Co–btx coordination polymers with novel topologies have been studied [15,16]. In addition, aromatic carboxylates such as 1,2,4,5-benzenetetracarboxylate, 1,3,5-benzenetricarboxylate, terephthalate, 5-substituted isophthalate, ligands are of particular interest due to their multi-carboxylate groups and the versatile coordination modes of these carboxylate groups, such as monodentate, bis-monodentate or chelating modes, leading to diverse structures of the resulting MOCPs [17]. The combination of flexible btx and aromatic polycarboxylate ligands may induce novel architectures and versatile properties. Wang and co-workers have presented a rare example of entangled coordination polymer containing both interpenetrating and polythreading features coordination polymer $[\text{Zn}(\text{CH}_3\text{O-ip})(\text{btx})]_2 \cdot \text{H}_2\text{O}$ ($\text{CH}_3\text{O-ip}$ = 5-methoxyisophthalate) [18]. We have reported three unprecedented binodal high-connected metal-organic frameworks constructed from btx and 1,2,4,5-benzenetetracarboxylate [19,20]. As a part of our ongoing studies on ternary transition metal complexes based on btx and aromatic carboxylate ligands, two new coordination polymers with interesting luminescence properties were prepared and structurally characterized. $[\text{Ni}(\text{btx})(\text{nip})(\text{H}_2\text{O})]_n$ (**1**) (H_2nip = 5-nitroisophthalic acid, H_2mip = 5-methyisophthalic acid) reveals a 3-fold interpenetrating 3D CdSO_4 -type network, while $[\text{Cd}(\text{btx})(\text{mip})(\text{H}_2\text{O})]_n \cdot \text{H}_2\text{O}$ (**2**) shows a 2D (4, 4) sheet-like network, which is finally extended into a 3D **3,5T1** supramolecular framework through multiple strong hydrogen bond interactions. To the best of our knowledge, coordination polymers exhibiting such **3,5T1** supramolecular network have only rarely been reported [21].

Experimental

Materials and measurements

All reagents were obtained from commercial sources and used without further purification. The ligand btx was prepared according to literature procedures [22]. Elemental analysis (C, H, and N) was performed on a Perkin–Elmer 240C Elemental Analyzer. Power X-ray diffraction (XRD) data were recorded on a Rigaku D/Max-2500 diffractometer at 40 kV, 100 mA for a Cu-target tube and a graphite monochromator. FT-IR spectra were recorded on an Avatar 360 (Nicolet) spectrophotometer between 400 and 4000 cm^{-1} , using the KBr pellet method. Thermogravimetric analyses (TGA) were conducted on a Netzsch TG 209 thermal analyzer in N_2 environmental at a heating rate of 10 $^\circ\text{C}/\text{min}$ up to 800 $^\circ\text{C}$. The fluorescence spectra were collected with a Hitachi F-4500 spectrophotometer at room temperature.

Preparation of the complexes **1** and **2**

$[\text{Ni}(\text{btx})(\text{nip})(\text{H}_2\text{O})]_n$ (**1**)

A mixture of $\text{Ni}(\text{CH}_3\text{COO})_2 \cdot 4\text{H}_2\text{O}$ (0.1 mmol, 24.9 mg), btx (0.1 mmol, 24.0 mg), H_2nip (0.1 mmol, 105.5 mg) was added in 20 mL H_2O . It was then sealed in a 25 mL Teflon-lined stainless steel autoclave and heated at 160 $^\circ\text{C}$ for 3 days; then, the reaction system was cooled to room temperature at 5 $^\circ\text{C}/\text{h}$. Green block-shaped crystals were collected by filtration and washed with distilled water in 45% yield (based on $\text{Ni}(\text{CH}_3\text{COO})_2 \cdot 4\text{H}_2\text{O}$). Anal. Calcd. for $\text{C}_{20}\text{H}_{17}\text{N}_7\text{NiO}_7$ (%): C, 45.66, H, 3.26, N, 18.64. Found (%): C, 45.32, H, 3.12, N, 18.39. IR (KBr, cm^{-1}): 3420(vs), 3120(w), 2368(w), 1617(s), 1532(s), 1461(s), 1353(s), 1282(s), 1125(w), 733(w), 677(w).

$[\text{Cd}(\text{btx})(\text{mip})(\text{H}_2\text{O})]_n \cdot \text{H}_2\text{O}$ (**2**)

The synthetic procedure of **2** was analogous to the synthesis of **1**, except that H_2nip and $\text{Ni}(\text{CH}_3\text{COO})_2 \cdot 4\text{H}_2\text{O}$ were used instead of H_2mip (0.1 mmol, 18.0 mg) and $\text{Cd}(\text{CH}_3\text{COO})_2 \cdot 2\text{H}_2\text{O}$ (0.1 mmol, 26.7 mg), respectively. Colorless block-shaped crystals of **2** (yield: 43%) could be obtained. Anal. Calcd. for $\text{C}_{21}\text{H}_{22}\text{CdN}_6\text{O}_6$ (%): C, 44.50, H, 3.91, N, 14.83. Found (%): C, 44.36, H, 3.82, N, 14.55. IR (KBr, cm^{-1}): 3427(vs), 3103(w), 2948(w), 1640(s), 1542(s), 1483(s), 1348(s), 1284(w), 1064(s), 733(w), 683(w).

X-ray crystallography

The crystallographic data for the single crystal of compound **1** was collected at 100 K on an Agilent SuperNova Dual Source diffractometer with Atlas CCD detector, microfocus sources and focusing multilayer optics, using Mo $K\alpha$ radiation ($\lambda = 0.71073$ Å). CrysAlis PRO [23] software was used to collect, index, scale and apply analytical absorption correction based on faces of the crystal with multi-scan mode. X-ray diffraction data for **2** was collected on a Bruker Smart 1000 CCD diffractometer using graphite-monochromated Mo $K\alpha$ radiation ($\lambda = 0.71073$ Å) at room temperature with ω -scan mode. A semi-empirical absorption correction was applied using the SADABS program [24]. Both structures were solved by direct methods with SHELXS-97 and refined by full-matrix least squares on F^2 with SHELXTL [25]. All non-hydrogen atoms were refined with anisotropic thermal parameters. The H-atoms of organic ligands were generated theoretically onto the specific atoms and refined isotropically. The aqua hydrogen atoms in **1** and **2** were located from difference Fourier maps and refined with isotropic displacement parameters. The crystallographic data for **1** and **2** are listed in Table 1, and selected length and angle parameters for **1** and **2** are presented in Table 2, respectively.

Results and discussion

Crystal structures

Crystal structures of compound **1**

The structure of **1** is a 3D MOF. X-ray analysis reveals that **1** crystallized in the monoclinic space group Cc. The asymmetric unit

Table 1
Crystal and refinement data for complexes **1** and **2**.

	1	2
Empirical formula	$\text{C}_{20}\text{H}_{17}\text{N}_7\text{NiO}_7$	$\text{C}_{21}\text{H}_{22}\text{CdN}_6\text{O}_6$
Formula weight	526.12	566.85
Crystal system	Monoclinic	Triclinic
Space group	Cc	P $\bar{1}$
<i>a</i> (Å)	16.1760(3)	10.2021(7)
<i>b</i> (Å)	16.9691(3)	11.4351(8)
<i>c</i> (Å)	7.3806(2)	11.8614(8)
α (deg)	90	69.2300(8)
β (deg)	94.459(2)	68.8065(8)
γ (deg)	90	67.0920(7)
<i>V</i> (Å ³)	2019.77(7)	1150.98(14)
<i>Z</i>	4	2
<i>D</i> _{calc} (g/m ³)	1.730	1.636
μ (mm ⁻¹)	1.025	0.999
<i>F</i> (000)	1080	572
Crystal size (mm)	0.28 × 0.21 × 0.15	0.27 × 0.23 × 0.22
Total reflections	21,862	7039
Unique reflections	4784	5062
<i>R</i> _{int}	0.0635	0.0164
GOF	0.851	1.002
<i>R</i> ₁ (<i>I</i> > 2σ(<i>I</i>))	0.0366	0.0254
<i>wR</i> ₂ (<i>I</i> > 2σ(<i>I</i>))	0.0805	0.0622
$\Delta\rho$ max (eÅ ⁻³)	0.393	0.341
$\Delta\rho$ min (eÅ ⁻³)	-0.330	-0.421

$$R_1 = \sum ||F_o| - |F_c|| / \sum |F_o|; wR_2 = \sum [w(F_o^2 - F_c^2)^2] / \sum [w(F_o^2)^2]^{1/2}.$$

Table 2
Selected bond lengths (Å) and angles (°) for complexes **1** and **2**.

Complex 1			
N1–Ni1	2.071(3)	O6A–Ni1–N4B	87.55(8)
Ni1–O1W	2.036(2)	N1–Ni1–N4B	172.08(10)
Ni1–O6A	2.056(2)	O1W–Ni1–O1	91.67(8)
Ni1–N4B	2.085(2)	O6A–Ni1–O1	171.97(8)
Ni1–O1	2.095(2)	N1–Ni1–O1	91.48(8)
Ni1–O2	2.229(2)	N4B–Ni1–O1	92.38(8)
O1W–Ni1–O6A	96.34(8)	O1W–Ni1–O2	152.91(8)
O1W–Ni1–N1	91.75(9)	O6A–Ni1–O2	110.75(7)
O6A–Ni1–N1	87.66(8)	N1–Ni1–O2	89.25(8)
O1W–Ni1–N4B	95.04(9)	N4B–Ni1–O2	86.55(8)
Complex 2			
Cd1–O3A	2.2953(17)	O3A–Cd1–O1W	129.60(7)
Cd1–N3	2.2957(19)	N3–Cd1–O1W	83.97(8)
Cd1–N6	2.301(2)	N6–Cd1–O1W	86.28(8)
Cd1–O2	2.3228(15)	O2–Cd1–O1W	146.40(7)
Cd1–O1W	2.3445(18)	O3A–Cd1–O1	137.38(5)
Cd1–O1	2.5275(15)	N3–Cd1–O1	86.55(6)
Cd1–O4A	2.5707(17)	N6–Cd1–O1	85.56(7)
N6–Cd1–O2	91.31(7)	O2–Cd1–O1	53.66(5)
O1–Cd1–O4A	169.55(5)	O1W–Cd1–O1	92.76(6)
O3A–Cd1–N3	92.80(7)	O3A–Cd1–O4A	52.88(5)
O3A–Cd1–N6	99.88(8)	N3–Cd1–O4A	91.23(7)
N3–Cd1–N6	167.14(7)	N6–Cd1–O4A	94.70(7)
O3A–Cd1–O2	83.84(6)	O2–Cd1–O4A	136.70(6)
N3–Cd1–O2	92.18(7)	O1W–Cd1–O4A	76.85(7)

Symmetry transformations used to generate equivalent atoms in **1**: A $x + 1/2$, $-y + 1/2$, $z + 1/2$; B $x + 1/2$, $y + 1/2$, $z - 1$. In **2**: A $x - 1$, y , z ; B $x + 1$, y , z .

of **1** contains one Ni(II) cation, one btx ligand, one nip anion and one coordinated water molecule. As depicted in Fig. 1a, the coordination sphere around the six-coordinated Ni(II) ion is composed of two nip²⁻ ligands, one water and two btx ligands. The equatorial plane is formed by two chelating carboxylate oxygen atoms (O1 and O2) from one nip²⁻, one bis-monodentate carboxylate oxygen atom (O6) from a symmetry-equivalent nip²⁻ and one oxygen atom from a coordinated aqua molecule (O1W). The apical positions are occupied by two nitrogen atoms (N1 and N4B) from two distinct btx ligands ($B = x + 1/2, y + 1/2, z - 1$). The Ni–O bond distances are in the range of 2.038(2)–2.229(2) Å, and the Ni–N bond distances are 2.073(3) and 2.084(3) Å, respectively, which are all similar to those found in other Ni(II) compounds [26].

In **1**, the btx ligands adopt a *trans*-conformation and bridge the adjacent two Ni(II) centers to assemble into an infinite 1D [Ni(btx)]_n ribbon-like chain along the *b* direction, wherein the intra-chain adjacent Ni···Ni separation is 14.183(3) Å. For the btx containing N1 and N4, the dihedral angles between the triazole ring and the phenyl plane are 71.851(9)° and 63.191(1)°, respectively. The torsion angle (C5–C4–C3–N3) is 48.906(4)° for the former kind of btx, whereas the corresponding torsion angle (C6–C7–C12–N5) is enhanced to 68.077(3)° for the latter type of btx. The flexible skeleton is conducive to such conformational transformation. Moreover, nip anions exhibit bridging ligands with one monodentate carboxylic group and one chelating carboxylic group to connect two Ni(II) ions, generating a 1D zigzag [Ni(nip)(H₂O)]_n neutral chain along the *a* direction. Two kinds of chains are interconnected along different directions to generate a 3D framework (Fig. 1b). As for the topological geometry, each Ni(II) ion connecting four neighboring Ni(II) ions can be considered as 4-connected node, btx and nip²⁻ bridging ligands can be regarded as linkers, thus the structure of **1** can be simplified into a (6⁵.8)-cdfs topology. Because the single 3D cdfs network has large spacious voids, it allows two other identical cdfs networks to interpenetrate giving rise to a 3-fold interpenetrating 3D cdfs network (Fig. 1c). In addition, one classical O–H···N hydrogen bond interaction between the coordinated water molecule and 2-position triazole nitrogen atoms (O1W···N2 = 2.879(3) Å, O1W–H1W···N2 = 161°)

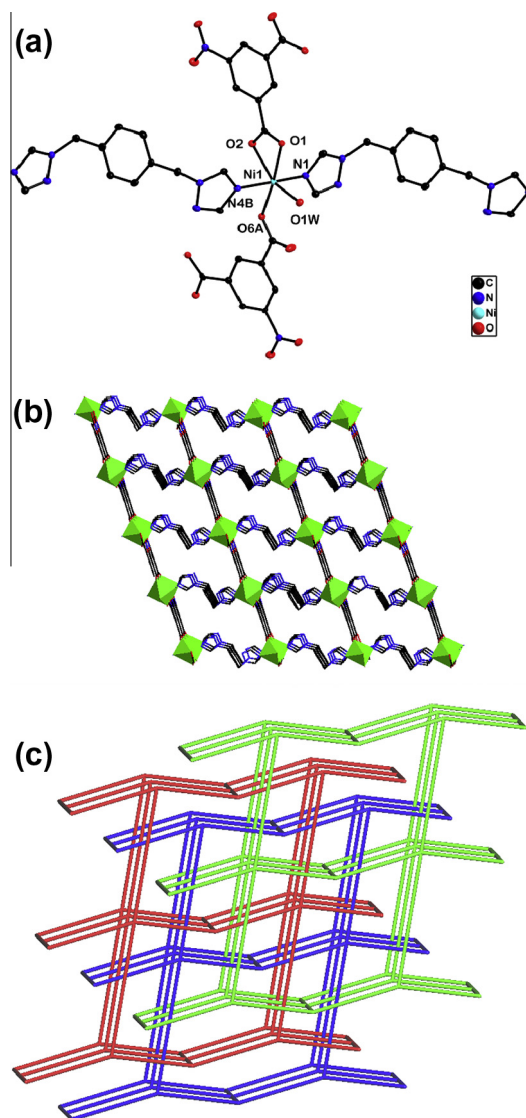


Fig. 1. (a) The coordination environment for Ni(II) ion in complex **1**, showing thermal displacement ellipsoids at the 30% probability level. (b) Perspective view of the 3D framework for complex **1**. (c) 3D framework with 4-connected cdfs topology.

contribute to the stability of the resultant three dimensional supramolecular framework **1**.

Crystal structures of compound **2**

Compound **2** is a 3,5-connected binodal 3D supramolecular network and crystallized in the space group of *P* $\bar{1}$. The asymmetric unit of **2** consists of one Cd(II) ion, one mip anion, one btx ligand, one coordination and one lattice water molecules. As depicted in Fig. 2a, each Cd(II) ion coordinates to two bridging btx ligands through N-coordination (Cd–N3 = 2.296(2) Å, Cd–N6 = 2.301(2) Å) in an almost linear configuration (N3–Cd–N6 = 167.143(7)°), two chelating mip²⁻ carboxylate oxygen atoms (the bond lengths of Cd–O range from 2.295(2) to 2.571(2) Å) and one H₂O solvate oxygen atom to form a pentagonal bipyramid geometry. Two conformational btx ligands act as bidentate *trans*-configuration ligands in which the dihedral angles between two triazole ring planes of btx ligand are 73.9° and 75.9°, respectively. The btx ligands link Cd(II) ions to form a 1D zigzag [Cd(btx)]_n cation chain. The adjusted 1D chains are parallel to each other and further connected by bis-chelating mip²⁻ ligands to assemble into a 2D (4, 4) grid structure, in which each 42-member parallelogram consists of four Cd(II)

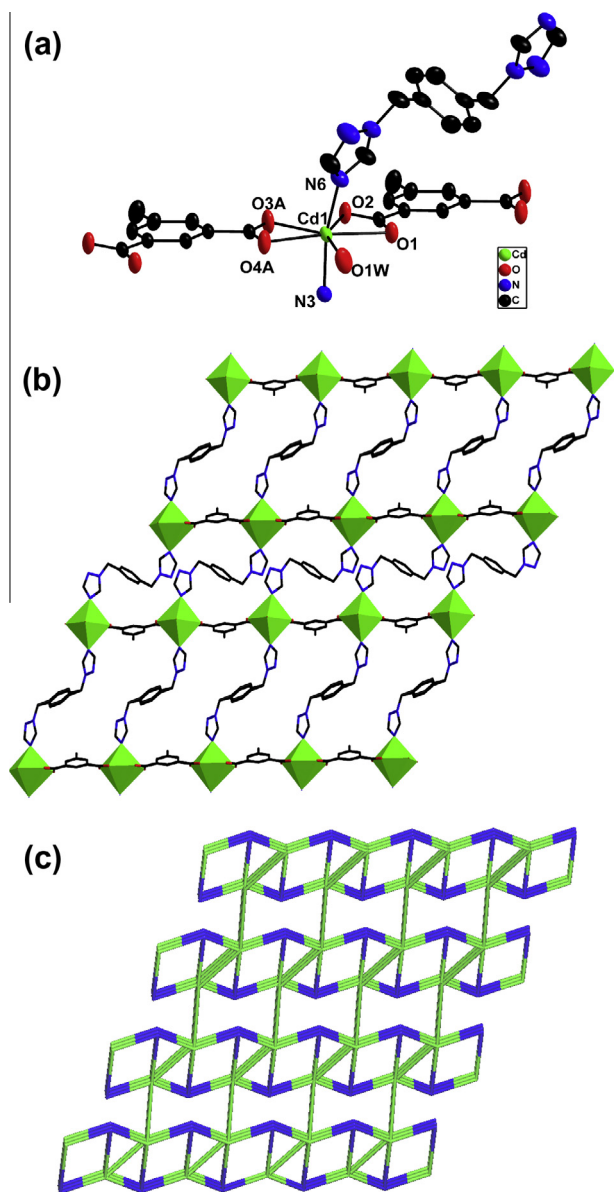


Fig. 2. (a) Local coordination geometry of the central Cd(II) cation in the complex **2**, showing thermal displacement ellipsoids at the 30% probability level. All hydrogen atoms are omitted for clarity. (b) 2D 4-connected grid structure consisting of 1D btx line chains. (c) 3D framework with binodal (3, 5)-connected **3,5T1** topology.

ions at the corners connected by two btx ligands and two mip^{2-} ligands. In each parallelogram, the Cd...Cd distances are 14.717(7) or 13.085(7) Å bridged by distinct conformational btx ligands, 10.202(7) Å separated by mip^{2-} ligands, respectively (Fig. 2b). More interesting, the neighboring (4, 4) layers are extended to a 3D supramolecular framework by three kinds of O—H...O hydrogen bond modes between water molecules and carboxylate oxygen atoms. One mode of hydrogen bonds is formed between the coordinated water molecules and chelating carboxylate oxygen atoms with O1W...O1 distance of 2.711(3) Å, a second mode is assembled between lattice water molecules and chelating carboxylate oxygen atoms with O2W...O4 distance of 2.912(4) Å and 2.817(4) Å, and a third mode is built between the coordinated water and lattice water molecules with O1W...O2W distance of 2.855(5) Å. The related hydrogen-bonding geometries are given in Table 3. For a topological view, each Cd(II) ion links five neighboring Cd(II) ions, which can be regarded as a 5-connected node, each mip^{2-} ligand

Table 3
Hydrogen-bonding geometry for **2**.

D—H...A	D—H (Å)	H...A (Å)	D...A (Å)	D—H...A (°)
O1W—H1A...O1	0.83(4)	1.90(4)	2.711(3)	169(4)
O1W—H1B...O2 W	0.82(3)	2.04(3)	2.855(5)	170(4)
O2W—H2A...O4	0.82	2.22	2.912(4)	141
O2W—H2B...O4	0.82	2.00	2.817(4)	171

Symmetry transformations used to generate equivalent atoms in **2**: A $x - 1, y, z$; B $x + 1, y, z$.

connect two Cd(II) ions and one mip^{2-} can be considered as a 3-connected node, and each btx ligand act as linker, giving a (3,5)-connected dinodal 3D **3,5T1** supramolecular network (Fig. 2c). To the best of our knowledge, only few complexes with this topology have been reported [21].

Comparison of complexes **1** with **2**

The above structural descriptions clearly reveal that it was evident that the coordination geometries of the central metal ions and the coordination modes of the organic ligands have an important on the formation and dimensions of the final structures. Comparison of complexes **1** with **2**, the coordination geometries of metal centers may play a crucial key role in determining the dimension of the resulting structures. The nickel atom in **1**, centers a [NiO₄N₂] octahedral coordination geometry, while [CdO₃N₂] in **2** with a pentagonal bipyramid geometry (The coordination sphere of **1** and **2** both contain one coordinated water molecule). Meanwhile, the 5-substituted isophthalates ligands adopt two different coordination modes as a $\mu_2-\eta^2:\eta^1$ coordination mode for nip^{2-} ligand in **1**, one $\mu_2-\eta^2:\eta^2$ coordination pattern connecting two Cd(II) atoms for mip^{2-} in **2**. As a result, the nip^{2-} ligand links the Ni(II) centers together to form a 1D ribbon-like polymeric chain in **1**, while a zig-zag polymeric chain in **2**. These chains are further extended by btx ligand to produce 3D or 2D network.

IR and XPRD

There is no absorption peak between 1760–1680 cm^{-1} for **1** and **2**, indicating that all carboxyl groups of the organic moieties are deprotonated [27]. The strong peaks at 1617 cm^{-1} and 1461 cm^{-1} for **1**, and 1640 cm^{-1} and 1483 cm^{-1} for **2** may be attributed to the asymmetric and symmetric vibrations of carboxylate groups. $\Delta\nu[v_{as}(COO)-\nu_s(COO)]$ are 156 cm^{-1} and 157 cm^{-1} , indicating bridging coordination of the carboxylate group to the metal center [28]. For **1** and **2**, the strong broad bands center at around 3000–3500 cm^{-1} , contributing to the O—H stretching vibration modes of water molecules or hydrogen bonds. The IR spectrum determination shows that $\nu_{as}(C=N)$ and $\nu_{as}(N=N)$ of the triazole ring vibrations in **1** and **2** are at 1532 cm^{-1} and 1282 cm^{-1} , 1542 cm^{-1} and 1284 cm^{-1} , respectively [29].

The simulated and experimental XRPD patterns of two polymers, obtained at room temperature, are shown in Fig. 3a and b. Their peak positions are in good consistency with each other, indicating the phase purity of the as-synthesized samples.

Thermal and photoluminescent properties

Thermogravimetric experiments under nitrogen atmosphere were carried out to investigate the thermal stability of two complexes. **1-2** possessed a two-step weight loss process, which was performed in the curves of TG and DTG (Fig. 4a and b). The first-step occurred from 216 °C to 285 °C with a weight loss of 3.54% for **1** and 110 °C to 140 °C with a weight of 6.43% for **2**, which can be attributed to the dehydration of the crystallized water molecules (calcd.: 3.43% for **1**, 6.36% for **2**). While the second step

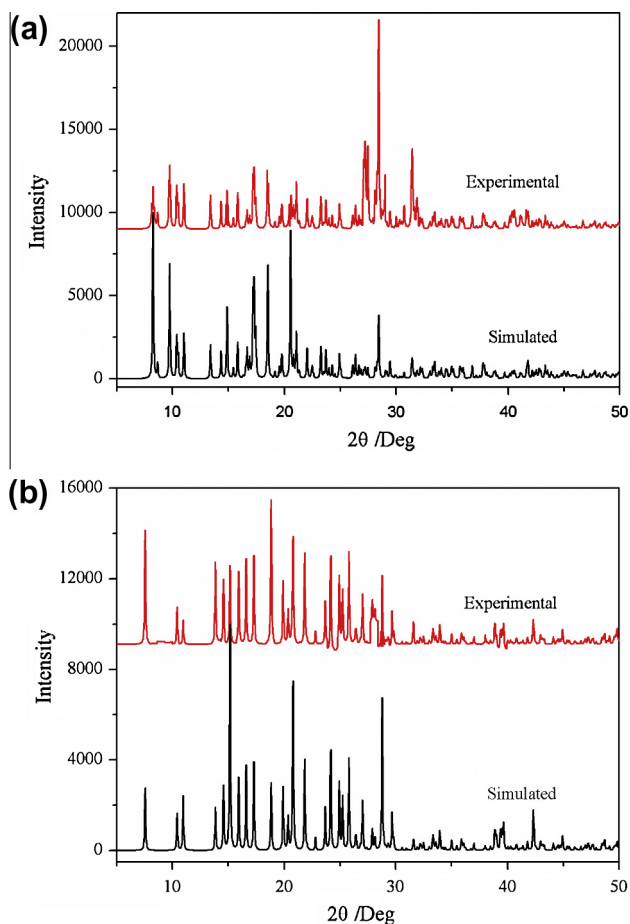


Fig. 3. (a and b) The powder X-ray diffraction patterns calculated from the single-crystal data and that obtained from the experiments for polymer **1** and **2**, respectively.

occurred in a temperature range from 346 °C to 668 °C for complex **1** and 280 °C to 521 °C for complex **2**, corresponding to the release of the btx and aromatic acid ligands and indicating the complete decomposition of complexes with 85.20% for **1** and 77.15% for **2**, residual weight corresponds to MO ($M = \text{Ni}$ or Cd) (calcd.: 85.8% for **1**, 77.35% for **2**). A comparison of the two complexes indicates that complex **1** is more stable than **2**. That is because the nickel atomic radius is smaller than the atomic radius of cadmium, which leads to the nickel binding capacity being much stronger than cadmium.

It is well known that inorganic–organic hybrid coordination compounds, especially with d^{10} metal centers, have been found to present photoluminescent properties and may have potential application as fluorescence-emitting materials [30,31]. The photoluminescent properties of complex **1–2** along with btx in the solid state at room temperature have been investigated (Fig. 5). The btx ligand exhibits an intense emission with a maximum at 432 nm upon excitation at 365 nm. The emission band of complex **1** appears in 430 nm ($\lambda_{\text{ex}} = 300$ nm), since it is similar to that of btx, the emission can probably be assigned to the intraligand transition of coordinated btx ligands. Obviously, large blue shifted emission occurs in **2** ($\lambda_{\text{em}} = 350$ nm, $\lambda_{\text{ex}} = 270$ nm) with respect to the free btx ligand and such broad band may be tentatively attributable to ligand-to-metal charge transfer (LMCT) as reported 2D cadmium(II) metal–organic frameworks [32]. However, the emission bands of the carboxylate ligands originated from the $n-\pi^*$ transition are weak, and it is considered that the carboxylate ligands have no significant contribution to the fluorescence emission of complexes **1** and **2** in the presence of the N-donor ligand [33].

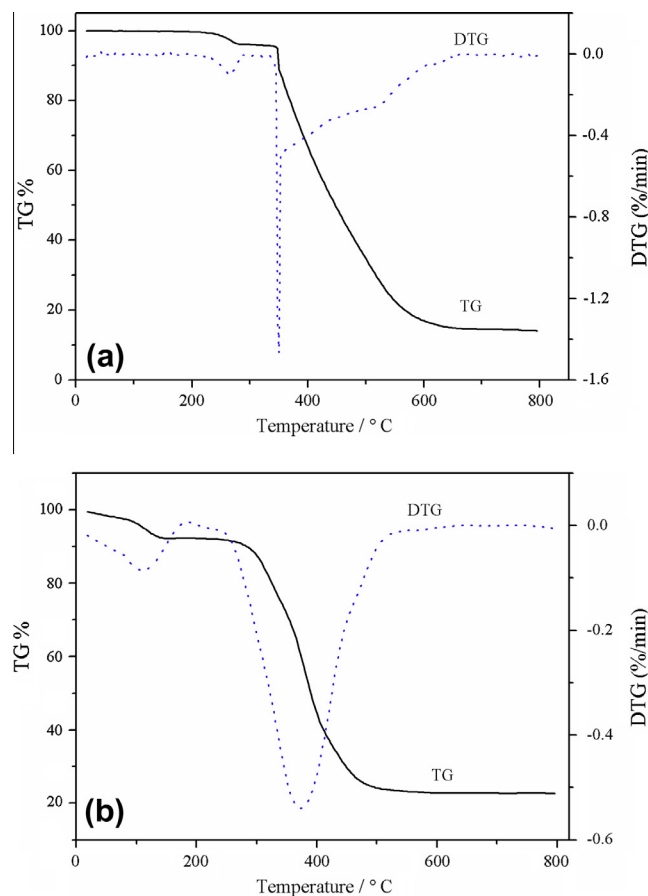


Fig. 4. (a and b) The TG and DTG curves of polymer **1–2** measured in N_2 atmosphere.

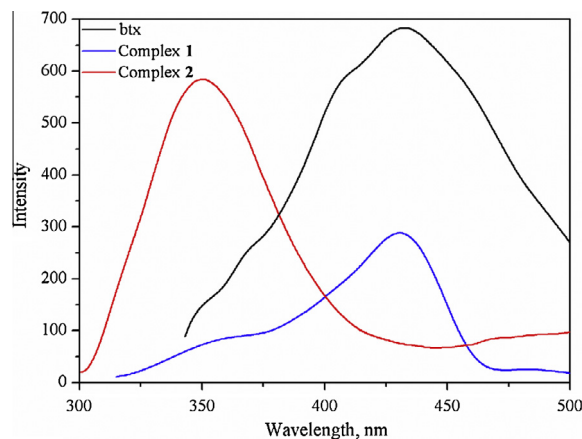


Fig. 5. Emission spectra of complex **1–2** and the free btx ligand.

Conclusion

Two new coordination polymers have been successfully isolated under hydrothermal conditions by reactions of two 5-substituted isophthalate, btx and metal salt. Complex **1** forms a 3-fold interpenetrating 4-connected 6^5 , 8-cds 3D network. Complex **2** exhibits a 3D supramolecular network. The structural differences of complexes **1** and **2** may result from the different coordination geometry of metal ions, and the distinct 5-substituted group with isophthalate ligands may impose remarkable steric and/or electronic effects on the coordination modes of organic carboxylate

ligands, which play crucial roles in the formation of the resulting coordination and/or supramolecular framework [34].

Acknowledgement

KVH thanks the Hercules Foundation (Project AUGE/11/029 “3D-SPACE: 3D Structural Platform Aiming for Chemical Excellence”) for funding.

Appendix A. Supplementary material

CCDC 972189 and 972187 contain the supplementary crystallographic data for the complexes **1** and **2**. These data can be obtained free of charge via <http://www.ccdc.cam.ac.uk/conts/retrieving.html>, or from the Cambridge Crystallographic Data Centre, 12 Union Road, Cambridge CB21EZ, UK; fax: +44 1223 336 033; or e-mail: deposit@ccdc.cam.ac.uk. Supplementary data associated with this article can be found, in the online version, at <http://dx.doi.org/10.1016/j.saa.2014.03.025>.

References

- [1] R.F. Song, Y.B. Xie, J.R. Li, X.H. Bu, Dalton Trans. (2003) 4742–4748.
- [2] C.H. Jiao, C.H. He, J.C. Geng, G.H. Cui, J. Coord. Chem. 65 (2012) 2852–2861.
- [3] L. Qin, S.L. Xiao, X.H. Zheng, G.H. Cui, Inorg. Chem. Commun. 34 (2013) 71–74.
- [4] W.C. Yang, Z.B. Zheng, H.L. Sun, K.Z. Wang, Spectrochim. Acta Part A: Mol. Biomol. Spectrosc. 86 (2012) 187–190.
- [5] Y. Bai, J.L. Wang, D.B. Dang, Y.N. Zheng, Spectrochim. Acta Part A: Mol. Biomol. Spectrosc. 97 (2012) 105–110.
- [6] B. Xu, X. Ji, Y. Cai, L. Li, G. Liu, C. Li, J. Mol. Struct. 52–55 (2014) 1056–1057.
- [7] A.X. Tian, X.J. Liu, J. Ying, D.X. Zhu, X.L. Wang, J. Peng, CrystEngComm 13 (2011) 6680.
- [8] B. Ding, Y.Y. Liu, Y.Q. Huang, W. Shi, P. Cheng, D.Z. Liao, S.P. Yan, Cryst. Growth Des. 9 (2009) 593.
- [9] J. Hu, J. Li, J.A. Zhao, H. Hou, Y. Fan, Inorg. Chim. Acta 362 (2009) 5023–5030.
- [10] S.Y. Zhang, Z.J. Zhang, W. Shi, B. Zhao, P. Cheng, D.Z. Liao, S.P. Yan, Dalton Trans. 40 (2011) 7993.
- [11] Y. Chen, S.Y. Zhang, X.Q. Zhao, J.J. Zhang, W. Shi, P. Cheng, Inorg. Chem. Commun. 13 (2010) 699–702.
- [12] L. Qin, X.H. Zheng, S.L. Xiao, G.H. Cui, Transition Metal Chem. 34 (2013) 71–74.
- [13] C.C. Wang, P. Wang, G.L. Guo, Transition Metal Chem. 38 (2013) 891–897.
- [14] L.F. Ma, X.K. Huo, L.Y. Wang, J.G. Wang, Y.T. Fan, J. Solid State Chem. 180 (2007) 1648–1657.
- [15] X.R. Meng, Y.L. Song, H.W. Hou, H.Y. Han, B. Xiao, Y.T. Fan, Y. Zhu, Inorg. Chem. 43 (2004) 3528–3536.
- [16] B.L. Li, Y.F. Peng, B.Z. Li, Y. Zhang, Chem. Commun. (2005) 2333–2335.
- [17] J.S. Lucas, L.D. Bell, C.M. Gandolfo, R.L. LaDuca, Inorg. Chim. Acta 378 (2011) 269–279.
- [18] J.H. Qin, L.F. Ma, Y. Hu, L.Y. Wang, CrystEngComm 14 (2012) 2891–2898.
- [19] J.M. Hao, L.N. Wang, K. Van Hecke, G.H. Cui, Inorg. Chem. Commun. 41 (2014) 43–46.
- [20] G.H. Cui, C.H. He, C.H. Jiao, J.C. Geng, V.A. Blatov, CrystEngComm 14 (2012) 4210.
- [21] M.D. Zhang, L. Qin, H.T. Yang, Y.Z. Li, Z.J. Guo, H.G. Zheng, Cryst. Growth Des. 13 (2013) 1961–1969.
- [22] B.F. Hoskins, R. Robson, D.A. Slizys, J. Am. Chem. Soc. 119 (1997) 2952.
- [23] Agilent Technologies CrysAlis PRO Agilent Technologies, Yarnton, England, 2012.
- [24] G.M. Sheldrick, SADABS, University of Göttingen, Germany, 1996.
- [25] G.M. Sheldrick, Acta Cryst. A64 (2008) 112–122.
- [26] M.A. Ali, M.A. Huq, M.H.S.A. Hamid, S.I. Chin, S.L. Pei, P.V. Bernhardt, Inorg. Chem. Commun. 13 (2010) 1445–1447.
- [27] B. Tao, W. Lei, F.R. Cheng, H. Xia, Bull. Korean Chem. Soc. 33 (2012) 1929.
- [28] G.B. Deacon, R.J. Phillips, Coord. Chem. Rev. 33 (1980) 227.
- [29] J.C. Geng, L. Qin, C.H. He, G.H. Cui, Transition Metal Chem. 37 (2012) 579–585.
- [30] F.H. Zhao, Y.X. Che, J.M. Zheng, Inorg. Chem. Commun. 24 (2012) 200–204.
- [31] Y.T. Wang, Y. Xu, Y.T. Fan, H.W. Hou, J. Solid State Chem. 182 (2009) 2707–2715.
- [32] S. Lin, L.J. Chen, H.H. Xu, J.B. Su, H. Huang, Inorg. Chem. Commun. 13 (2010) 1347–1349.
- [33] Y.W. Li, H. Ma, Y.Q. Chen, K.H. He, Z.X. Li, X.H. Bu, Cryst. Growth Des. 12 (2012) 189–196.
- [34] M. Du, C.P. Li, C.S. Liu, S.M. Fang, Coord. Chem. Rev. 257 (2013) 1282–1305.